HHS Public Access

Author manuscript

Nat Immunol. Author manuscript; available in PMC 2010 July 01.

Published in final edited form as:

Nat Immunol. 2010 January ; 11(1): 83–89. doi:10.1038/ni.1826.

Different routes of bacterial infection induce long-lived T_H1 memory cells and short-lived T_H-17 cells

Marion Pepper[1,2], **Jonathan L Linehan**[1,2], **Antonio J Pagán**[1], **Traci Zell**[1], **Thamotharampillai Dileepan**[1], **P. Patrick Cleary**[1], and **Marc K Jenkins**[1]

[1]Department of Microbiology, Center for Immunology, University of Minnesota Medical School, Minneapolis, MN, USA, 55455, Phone: 612-626-2715, Fax: 612-625-2199

Abstract

A sensitive peptide-major histocompatibility complex II (pMHCII) tetramer-based method was used to determine whether $CD4^+$ memory T cells resemble the T_H1 and T_H-17 subsets described *in vitro*. Intravenous or intranasal *Listeria monocytogenes* infection induced pMHCII-specific $CD4^+$ naïve T cells to proliferate and produce effector cells, about 10% of which resembled T_H1 or T_H-17 cells, respectively. T_H1 cells were also present among the memory cells that survived three months post-infection whereas T_H-17 cells disappeared. The short lifespan of T_H-17 cells was associated with low amounts of Bcl-2, interleukin 15 receptor, CD27 and little homeostatic proliferation. These results suggest that T_H1 cells induced by intravenous infection are more efficient at entering the memory pool than T_H-17 cells induced by intranasal infection.

Keywords

$CD4^+$ T lymphocyte; immunological memory; CD27; CCR7; *Listeria monocytogenes*; T_H1; T_H-17

Vaccination or prior encounter with a microbe generally results in immunity from subsequent infection with that microbe. This immunity is mediated by memory T and B cells, which are generated from naïve precursors following exposure to microbial antigens. T cell antigen receptor (TCR) binding to microbe-derived peptide-major histocompatibility complex (pMHC) ligands causes naïve T cells to proliferate and differentiate into effector cells capable of producing microbicidal cytokines1. Although ~90% of the effector cells die, some survive to become long-lived memory cells capable of a rapid and protective response to re-infection with the relevant microbe2.

Two major subsets of memory T cells have been described, central (T_{cm}) and effector memory cells (T_{em})3–5. T_{cm} express CCR7 [http://www.signaling-gateway.org/molecule/

Correspondence should be addressed to M.K.J. (jenki002@umn.edu).

[2]These authors contributed equally to this work.

Author contributions M. P. designed the study, did experiments, analyzed data, and wrote the manuscript, J. L. L, A. J. P., T. Z., and D. T. did experiments, P. P. C. designed experiments, and M. K. J. designed the study, analyzed data, and wrote the manuscript.

query?afcsid=A000630] and L-selectin, allowing for recirculation through lymph nodes. T_{em} lack CCR7 and L-selectin yet express other homing receptors needed for migration into non-lymphoid organs6. When stimulated with antigen, T_{em} are immediately capable of effector cytokine production and cytolysis, whereas T_{cm} proliferate to produce new effector cells, which then acquire these functions. Heterogeneity in lymphokine production potential also exists in the case of $CD4^+$ T cells. Naïve $CD4^+$ T cells differentiate into T_H1, T_H2 or T_H-17 effector cells when stimulated *in vitro* with antigen and specific combinations of cytokines7. In addition, certain infections induce $CD4^+$ effector cells with the properties of T_H1 or T_H2 cells8.

However, it is still not clear that pMHCII-specific $CD4^+$ memory T cells exist as discrete T_H1, T_H2 or T_H-17 subsets *in vivo* because such cells are difficult to detect in normal hosts. To circumvent this problem, immune memory by $CD4^+$ T cells has been studied *in vitro*9 or *in vivo*1,10,11 by adoptive transfer of TCR transgenic T cells. These approaches are artificial in that memory T cells are generated from disrupted lymphoid tissue9–11 or are so abundant that normal homeostasis is perturbed12–14. Thus, it is not clear how well genuine polyclonal $CD4^+$ memory T cells fit into the T_H1, T_H2, T_H-17 or T_{cm} and T_{em} categories.

Here we addressed this problem with a sensitive pMHCII tetramer-based approach that allowed detection of polyclonal pMHCII-specific $CD4^+$ T cells in normal mice following *Listeria monocytogenes* infection. We found that intravenous and intranasal infection induced T_H1 and T_H-17 $CD4^+$ effector T cells, respectively, although the most abundant cells in both cases did not resemble any of the canonical T_H subsets. In addition, we found that T_H1 cells were much more likely than T_H-17 cells to enter the memory cell pool.

Results

Detection of pMHCII-specific $CD4^+$ memory T cells

A pMHCII tetramer-based approach was used to identify $CD4^+$ T cells specific for a pMHCII produced during bacterial infection. The pMHCII tetramer consisted of the I-A^b MHCII molecule bound to a variant of peptide consisting of amino acids 52–68 from the I-E alpha chain called 2W1S15. The 2W1S peptide is highly immunogenic in C57BL/6 (B6) mice because of a relatively large naïve population capable of recognizing 2W1S:I-A^b (ref. 16). B6 mice were infected with an attenuated strain of *L. monocytogenes* (ΔActA) engineered to secrete a fusion protein containing a portion of chicken ovalbumin and the 2W1S peptide (LM-2W1S)17 or a mycobacterial peptide ESAT6 (LM-ESAT6)18. These bacteria replicate for several days in mice and are then completely eliminated by innate and adaptive immune mechanisms19. Cells from each mouse were stained with a fluorochrome-labeled 2W1S:I-A^b tetramer and anti-fluorochrome magnetic beads at various times after infection and enriched on a magnetized column20. The bound fraction was then stained with antibodies specific for CD3, CD4, CD8, CD44 and a cocktail of non-T cell lineage-specific antibodies to aid in the identification of $CD4^+$ memory T cells.

Because effector and memory T cells express many of the same surface markers, the latter cells were identified as the population that stabilized after the expansion and contraction phases of the primary response21. Initial analyses involved standard intravenous infection.

Mice that were not infected contained a small population of about 300 2W1S:I-A^b-binding $CD3^+$ $CD4^+$ cells in the spleen and lymph nodes, the vast majority of which were $CD44^{lo}$ as expected for naïve cells (Fig. 1a). The tetramer bound to these T cells via the TCR as evidenced by the finding that no 2W1S:I-A^b-binding cells were detected among the $CD8^+$ MHCI-restricted T cells. Mice infected 7 days earlier with LM-ESAT6 also contained about 300 $CD44^{lo}$ 2W1S:I-A^{b+} $CD4^+$ naïve T cells (Fig. 1b). In contrast, mice infected with LM-2W1S 7 days earlier contained a large population of $CD44^{hi}$ 2W1S:I-A^{b+} $CD4^+$ T cells in the spleen and lymph nodes that could still be detected on day 190 and beyond. The 2W1S:I-A^b-specific $CD4^+$ T cells peaked at ~140,000 cells by day 5 after LM-2W1S infection and then declined rapidly to 20,000 cells by day 20 (Fig. 2). This contraction phase ended abruptly on day 20 after which the population slowly declined until day 250 with a half-life of about 40 days (Fig. 2). By day 250, only about 200 $CD44^{hi}$ 2W1S:I-A^{b+} $CD4^+$ T cells remained in the spleen and lymph nodes, and this number remained stable for the next 150 days. Although 2W1S:I-A^{b+} $CD4^+$ T cells were not detected in the bone marrow in uninfected mice (data not shown), about 1,500 $CD44^{hi}$ 2W1S:I-A^{b+} $CD4^+$ T cells appeared in the bone marrow by day 20 and then declined to 150 cells by day 300. Thus, 2W1S:I-A^b-specific $CD4^+$ T cells expanded to a peak number on day 5, contracted until day 20, and then entered a memory phase characterized by slow numerical decline for the next 230 days. In addition, some of the 2W1S:I-A^b-specific memory $CD4^+$ T cells were present in the bone marrow, although more were in the spleen and lymph nodes.

Infection route influences $CD4^+$ T cell differentiation

We next determined whether $CD4^+$ memory cells induced by intravenous infection resembled any of the canonical T_H subsets. Lymphokine production by 2W1S:I-A^b-specific $CD4^+$ memory cells was measured by direct *ex vivo* intracellular staining22 in mice that were infected 24 days before with LM-2W1S, and then challenged for 2 h with LM-2W1S or LM-ESAT6. Two hours was chosen because this is the time of maximal *in vivo* lymphokine production by antigen-experienced $CD4^+$ T cells stimulated by intravenous injection of peptide23 or infection with LM-2W1S (data not shown). 2W1S:I-A^b-specific $CD4^+$ memory cells did not express CD69 (Fig. 3a) or produce interferon-γ (IFN-γ) or interleukin 17A (IL-17A) after challenge with LM-ESAT6 (Figs. 3a,b). In contrast, about 30–40% of the memory cells produced IFN-γ after challenge (Fig. 3a,b) with LM-2W1S, while none of these cells produced IL-17A (Fig. 3b) or IL-5 (data not shown). The failure of the majority of 2W1S:I-A^b–specific $CD4^+$ memory cells to make IFN-γ after challenge was not related solely to a lack of 2W1S:I-A^b recognition after challenge since many of the cells expressed the TCR signal-dependent CD69 molecule but did not make IFN-γ (Fig. 3a). Therefore, about one-third of the 2W1S:I-A^b-specific $CD4^+$ memory cells induced by intravenous infection resembled T_H1 cells while the remainder did not produce any of the canonical T_H1, T_H2 or T_H-17 cytokines.

It was possible that many of the 2W1S:I-A^b-specific $CD4^+$ memory cells that were $CD69^+$ but were not making cytokines 2 h after challenge would have gone on to produce cytokines. To address this issue, spleen and lymph node cells from mice infected 22 days earlier with LM-2W1S were stimulated *in vitro* with the soluble TCR signal mimics phorbol myristate acetate (PMA) and ionomycin in the presence of an exocytosis inhibitor. IFN-γ-producing

cells peaked at about 50% of the total 2W1S:I-A^b-specific $CD4^+$ memory population between 3.5 and 6 h of stimulation (Fig. 3c). Since IFN-γ should accumulate under these conditions, these results indicated that only a subset of the 2W1S:I-A^b-specific $CD4^+$ memory cell population had IFN-γ production potential. This conclusion was supported by the finding that about 50% of the 2W1S:I-A^b-specific $CD4^+$ memory cells induced by intravenous infection expressed the T_H1-associated transcription factor T-bet24 before challenge, while none expressed the T_H-17-associated transcription factor RORγt25 (Fig. 3d) and none became $Foxp3^+$ regulatory T cells17. Since T-bet expression controls the T_H1 differentiation program in most cases24, this finding indicates that only a subset of the memory cells induced by intravenous infection had differentiated into T_H1 cells.

It was possible that the induction of T_H1 but not T_H-17 or T_H2 cells was related to the intravenous route of infection. We therefore studied the effect of intranasal administration of LM-2W1S organisms based on reports that IL-17A-producing T cells are induced during mucosal bacterial infections26,27. Indeed, we found that about 7% of the 2W1S:I-A^b-specific $CD4^+$ T cells in the spleen and lymph nodes of mice 24 days after intranasal LM-2W1S infection produced IL-17A, while very few produced IFN-γ, 2 h after challenge with LM-2W1S but not LM-ESAT6 (Fig. 3b). In addition, about 15% of the 2W1S:I-A^b-specific T cells induced by intranasal infection expressed RORγt, as evidenced by green fluorescent protein (GFP) expression in *Rorc(gt)*$^{+/GFP}$ mice or intracellular RORγt staining (Fig. 3d). These results demonstrate that intranasal LM-2W1S infection induced some of the 2W1S:I-A^b-specific T cells to differentiate into T_H-17 cells. However, as in the case of intravenous infection, the major population showed no evidence of committing to any canonical lineage.

T_H-17 cells are shorter-lived than T_H1 cells

We next measured the survival of IFN-γ- or IL-17A-producing T cells to determine if these subsets were equally efficient at entering the memory pool. Mice infected at various earlier times were challenged with an intravenous injection of LM-2W1S organisms to identify the lymphokine-producing cells. Intravenous LM-2W1S infection generated about 12,000 IFN-γ-producing 2W1S:I-A^b-specific effector T cells in the spleen and lymph nodes by day 7, which comprised about 10% of all 2W1S:I-A^b-specific T cells. At all times after the contraction phase, IFN-γ-producing cells accounted for about 25% of the 2W1S:I-A^b-specific memory cells (Fig. 4a). Therefore, IFN-γ-producing 2W1S:I-A^b-specific T cells were as good or better than non-IFN-γ-producing cells at entering the memory pool.

Intranasal infection induced a similar pattern of 2W1S:I-A^b-specific $CD4^+$ T cell expansion, contraction and memory cell formation as intravenous infection albeit to a lower extent (Fig. 4b). The reduced magnitude of this response was probably related to the fact that the nasal mucosal lymphoid tissues, which are the main sites of priming after intranasal infection28, contain many fewer naïve T cells than the spleen where priming occurs following intravenous infection. About 2,000 IL-17A-producing 2W1S:I-A^b-specific effector cells were present on day 7, which as in the case of IFN-γ-producing cells in intravenously infected mice, comprised about 10% of all 2W1S:I-A^b-specific T cells at this time. However, unlike IFN-γ-producing cells, IL-17A-producing 2W1S:I-A^b-specific cells were

progressively lost such that fewer than 10 cells (or 0.5% of all 2W1S:I-A^b-specific T cells) remained at day 110 post infection. Thus, IL-17A-producing cells did not enter the memory pool as efficiently as IFN-γ-producing cells.

CD27 marks functional heterogeneity in $CD4^+$ memory T cells

Additional markers were sought that could give clues about the differential longevity of IFN-γ- and IL-17A-producing $CD4^+$ T cells and determine if they fit the definition of T_{cm} or T_{em}. Previous work demonstrated that $CD8^+$ memory T cells can be divided based on expression of the tumor necrosis factor (TNF) receptor family member CD27 [http://www.signaling-gateway.org/molecule/query?afcsid=A000546]29,30. In addition, $CD8^+$ memory cells that lack expression of CD27 have been shown to be short-lived30–33. Therefore, we assessed expression of CD27 and CCR7, a marker used to distinguish T_{cm} or T_{em}3. Most of the IFN-γ^+ or T-bet^+ 2W1S:I-A^b-specific $CD4^+$ T cells present greater than 20 days after intravenous infection were $CCR7^{lo}$ $CD27^+$ (Fig. 5a,b). Although cells with this phenotype were also present amongst the IFN-γ^- or T-bet^- cells in the same mice, these populations also contained many $CCR7^{hi}$ $CD27^+$ and $CCR7^{hi}$ $CD27^-$ cells. In contrast, most of the IL-$17A^+$ 2W1S:I-A^b-specific $CD4^+$ T cells present after intranasal infection were $CCR7^{hi}$ $CD27^-$ (Fig. 5c), while the IL-$17A^-$ cells contained more $CCR7^{hi}$ $CD27^+$ and $CCR7^{hi}$ $CD27^-$ cells like the IFN-γ^- cells in intravenously infected mice. Although the RORγt^+ 2W1S:I-A^b-specific $CD4^+$ T cells contained $CCR7^{hi}$ $CD27^-$ cells as in the case of IL-17A-producing cells (Fig. 5d), the RORγt^+ populations also contained $CD27^+$ cells. Therefore, based on CCR7 expression, the T_H1 cells resembled T_{em} while the T_H-17 cells resembled T_{cm}.

The finding that IL-17A-producing $CD4^+$ T cells lacked CD27 and were short-lived caused us to explore whether all $CD27^-$ $CD4^+$ memory cells had this property. This possibility was tested in an adoptive transfer experiment involving total $CD4^+$ memory T cells since 2W1S:I-A^b-specific memory cells were too infrequent to detect reliably after transfer. Purified total $CD27^+$ or $CD27^-$ $CD4^+$ $CD44^+$ T cells were sorted from *L. monocytogenes*-infected B6 mice ($CD90.2^+$) and transferred into naïve B6.PL-$Thy1^a$ ($CD90.1^+$) recipients (Fig. 6a). The $CD27^+$ $CD4^+$ memory cells survived stably over a 14-day period after adoptive transfer, while purified $CD27^-$ $CD4^+$ memory cells declined by about 80% (Fig. 6b). Thus, $CD27^-$ $CD4^+$ memory T cells were short-lived compared to $CD27^+$ $CD4^+$ memory T cells. Although this observation was based on total $CD4^+$ memory cells, it correlated with the finding that a subset of $CD27^+$ 2W1S:I-A^b-specific $CD4^+$ memory T cells expressed larger amounts of the Bcl-2 survival protein than $CD27^-$ memory T cells of the same specificity (Fig. 6c).

Minimal homeostatic proliferation by $CD27^-$ $CD4^+$ T cells

It was also possible that poor homeostatic proliferation contributed to the short lifespan of $CD27^-$ $CD4^+$ memory T cells. This possibility was tested with a bromo-2-deoxyuridine (BrdU) labeling experiment. B6 mice were infected with LM-2W1S and 40 days later given BrdU in the drinking water for 2 weeks. About 10% of the 2W1S:I-A^b-specific $CD4^+$ memory T cells induced by intravenous or intranasal infection labeled with BrdU (Fig. 7a and data not shown). Among the 2W1S:I-A^b-specific $CD4^+$ memory T cells, about 15% of

the $CD27^+$ and only 3% of the $CD27^-$ cells labeled with BrdU (Fig. 7a,b). The homeostatic proliferation results correlated with expression of the beta chain of the IL-15 receptor (IL-15R; also known as CD122). CD122 was expressed on some $CD27^+$ $CD4^+$ but very few $CD27^-$ $CD4^+$ memory T cells (Fig. 7c). Together, these results showed that $CD27^-$ $CD4^+$ memory T cells were poor homeostatic proliferators, perhaps as a result of a lack of IL-15R expression.

To further test this hypothesis, mice were injected with IL-15–IL-15Rα complexes, which have been shown to be superagonists for IL-15R signaling *in vivo*34. Injection of IL-15–IL-15Rα complexes into B6 mice 40 days after intravenous LM-2W1S infection led to a ~30-fold increase in the fraction of 2W1S:I-A^b-specific $CD4^+$ memory cells that underwent homeostatic proliferation over a short 5 day BrdU labeling period, and the cells that proliferated were enriched for $CD27^+$ cells (Fig. 7d). These results indicate that a lack of IL-15R expression limits the homeostatic proliferation of $CD27^-$ $CD4^+$ memory T cells.

Discussion

We found that intravenous or intranasal infection with LM-2W1S induced polyclonal 2W1S:I-A^b-specific $CD4^+$ memory T cells. The emergence of memory-phenotype cells was preceded by robust expansion of naïve cells, which peaked in the secondary lymphoid organs about a week after infection. In both infections, the number of 2W1S:I-A^b-specific $CD4^+$ T cells declined rapidly after the peak. This contraction phase ended on day 20, after which the cells declined slowly. The abrupt change in survival observed at day 20 indicated that this is when the memory phase of this response begins. Most of the 2W1S:I-A^b-specific $CD4^+$ T cells induced by intravenous infection were in the secondary lymphoid organs during the memory phase, with many fewer in the bone marrow. Thus, the secondary lymphoid organs are the main reservoir of endogenous polyclonal $CD4^+$ memory T cells induced by intravenous bacterial infection, and not the bone marrow as described for TCR transgenic memory cells induced by peptide plus adjuvant immunization35.

Our results suggest that some but not all aspects of the T_H1 or T_H-17 and T_{em} or T_{cm} paradigms apply to all $CD4^+$ memory T cells. The IFN-γ-producing memory cells induced by the transient bacterial infections studied here resembled T_H1 and T_{em} cells because of immediate IFN-γ but not IL-17 production capability and lack of CCR7 expression3. Similarly, the IL-17A-producing cells induced by intranasal infection resembled T_H-17 and T_{em} cells because of immediate IL-17A but not IFN-γ production capability. However, these cells expressed CCR7 and thus were phenotypically similar to T_{cm} and were short-lived. In addition, the dominant population of memory cells induced by either infection route did not produce IFN-γ, IL-17A or IL-5 and were heterogeneous with respect to CCR7 and CD27 expression. Therefore, these cells did not fit easily into the T_H1, T_H2, T_H-17 or T_{cm} and T_{em} paradigms. These cells may be less differentiated and thus capable of becoming T_H1, T_H2 or T_H-17 cells following secondary infection. Alternatively, these cells could be highly differentiated cells that produce lymphokines other than those that define the classical subsets.

The tendency of different routes of infection to induce different memory cells may be related to the innate cytokine environments of the relevant secondary lymphoid organs. Anatomic constraints make it likely that naïve $CD4^+$ T cells first become activated in the nasal-associated mucosal lymphoid tissue following intranasal infection28. A previous study26 found that IL-17A-producing $CD4^+$ effector T cells are preferentially induced in mice exposed to *Francisella tularensis* organisms via the respiratory mucosa. Similarly, another study 27 showed that infection of the upper airway with *Streptococcus pneumoniae* organisms generated a population of IL-17A-producing $CD4^+$ T cells. Thus, it is possible that the environment within mucosal secondary lymphoid organs is especially conducive to the differentiation of IL-17A-producing T cells. Since IL-6 is required for differentiation of these cells36,37 it is noteworthy that dendritic cells from the intestinal mucosal tissue have been reported to be better IL-6 producers than splenic dendritic cells38. In addition, transforming growth factor-β, which is also essential for the differentiation of IL-17A-producing T cells, is abundant in the mucosal tissues39. Conversely, splenic dendritic cells are potent producers of IL-12 (ref. 40), which is required for the differentiation of IFN-γ-producing T cells41.

Our results confirm the idea that $CD4^+$ memory T cells decline slowly over time, at least in some cases. Previous work42 reported this finding for IFN-γ-producing $CD4^+$ memory T cells induced by lymphocytic choriomeningitis virus infection. We also found that the total population of 2W1S:I-A^b-specific $CD4^+$ memory T cells induced by intravenous bacterial infection including those with IFN-γ-production potential declined slowly with a half-life of about 40 days between days 20 and 250 of the memory phase. It is worth noting that the aforementioned viral infection42 and the bacterial infections studied here were cleared very quickly from the host. Thus, the decline of $CD4^+$ memory T cells described in both cases may be related to a lack of persistent antigen presentation. It will be of interest to determine if $CD4^+$ memory T cells also decline during persistent infections caused by organisms like *Salmonella typhimurium*43.

After day 250, the number of 2W1S:I-A^b-specific memory cells stabilized at a level that was only about twice that of the naïve level of 300 cells. This survival pattern was remarkably similar to that observed for polyclonal naïve T cells12. Thus, it is possible that many murine $CD4^+$ memory T cells do not live longer than their already long-lived naïve precursors.

The decline of $CD4^+$ memory T cells induced by transient infections is in contrast to the remarkable numerical stability of $CD8^+$ memory T cells42. Since IL-15 is important for the homeostatic proliferation of both types of memory cells44, it may be telling that most $CD4^+$ memory T cells induced by bacterial infection, especially those lacking CD27, did not express the IL-15R. It is therefore reasonable to suspect that a low rate of IL-15-driven homeostatic proliferation contributed to the numerical decline of the $CD4^+$ memory T cell populations observed in our experiments. Our finding that increasing the availability of IL-15 in the form of IL-15–IL-15Rα complexes increased the homeostatic proliferation of $CD4^+$ memory T cells is consistent with this possibility.

IL-17A-producing effector cells did not efficiently enter the memory cell pool. One possible explanation for this finding is that these cells simply lost the capacity to produce IL-17A37.

Alternatively, the IL-17A-producing cells could have died because of a lack of CD27. CD27–CD70 interactions have been shown to be important for the maintenance of $CD8^+$ memory cells31,45 perhaps via CD27 signaling through TRAF5 (ref. 46). The lack of a CD27 signal may have also lead to reduced expression of the anti-apoptosis protein Bcl-2 and a greater rate of apoptosis than that of $CD27^+$ $CD4^+$ memory cells. In contrast, IFN-γ-producing memory cells may gain a survival benefit from expression of T-bet, which has been reported to control CD122 expression and thus the capacity for IL-15-dependent homeostatic proliferation47. Against this scenario is the finding that T-bet expression is a marker of terminal differentiation and death in $CD8^+$ memory T cells48.

Our results also demonstrate an association between CD27 expression and lymphokine production potential. This finding adds to other evidence indicating that signaling through CD27 is causally related to acquisition of IFN-γ production potential49,50, perhaps by contributing to the induction of T-bet51. However, it is worth noting that about half of the $ROR\gamma t^+$ 2W1S:I-A^b-specific memory cells induced by intranasal infection expressed CD27 but did not produce IFN-γ or IL-17A, and could have been committed to IL-22 or IL-17F production52. Thus, CD27 may be necessary but not sufficient for IFN-γ production by $CD4^+$ memory cells and not permissive for IL-17A production. This possibility is supported by recent work indicating that $CD27^+$ γδ T cells cannot become IL-17-producing cells53.

Finally, our results have implications for protective immunity. Intranasal immunization of mice with *S. pneumoniae* organisms induces protective immunity that is dependent on IL-17A and $CD4^+$ T cells54. Our findings suggest that this immunity may be short-lived because IL-17A-producing $CD4^+$ effector T cells do not survive to become memory cells. Supporting this suggestion is the clinical observation that streptococcal infections, for example otitis media, tend to recur55.

Methods

Mice

Six- to eight-week-old B6, B6.129S6-*Tbx21*^{tm1Glm}/J, B6.129P2(Cg)-*Rorc*^{tm2Litt}/J and B6.PL-Thy1^a/CyJ mice were purchased from the Jackson Laboratory or National Cancer Institute (B6). All mice were housed in specific pathogen-free conditions in accordance with University of Minnesota and NIH guidelines. All animal experiments were approved by the Institutional Animal Care and Use Committee of the University of Minnesota.

L. monocytogenes infections

Mice were injected intravenously with 10^7 or intranasally with 10^9 *L. monocytogenes* organisms expressing a recombinant protein consisting of chicken ovalbumin fused to the 2W1S (EAWGALANWAVDSA)17 or ESAT6 (ref. 18) peptides. In some experiments, animals were challenged intravenously after the primary infection with 5×10^8 live LM-2W1S or LM-ESAT6. Challenged animals were sacrificed 2 h later for analysis.

BrdU labeling

To analyze homeostatic proliferation, mice were infected with LM-2W1S and at least 40 days later were given BrdU (0.8 mg/ml) in the drinking water for 12–14 d. In some cases, mice were injected intraperitoneally with complexes of recombinant mouse IL-15Rα–Fc chimera (7 μg per animal) and recombinant mouse IL-15 (1.5 μg per animal; both from R&D Systems) formed as described previously34,56. Animals were injected with IL-15–IL-15Rα complexes and BrdU (2 mg/animal by intraperitoneal injection) for 2 d and then BrdU was added to the drinking water (0.8 mg/ml) for an additional 3 d prior to harvesting spleen and lymph nodes and staining as described above.

Tetramer production

Biotin-labeled soluble 2W1S:I-A^b molecules were produced, expressed in drosophila S2 cells, purified and tetramerized with streptavidin (SA)-PE- or SA-APC (Prozyme) as described previously16,20.

Tetramer enrichment and flow cytometry

Spleen and lymph node cells or leg bone marrow cells were prepared, stained with 2W1S:I-A^b–SA-PE or SA-APC tetramer and PerCP-Cy5.5–anti-CCR7 (4B12) (eBioscience) at 25°C for 1 h and then with anti-PE and/or anti-APC magnetic beads. Bead-bound cells were then enriched on magnetized columns and a sample was removed for counting as described previously16. It was assumed that the leg bones contained $1/5^{th}$ of the bone marrow in the body57. All antibodies were from eBioscience unless otherwise noted. The rest of the sample underwent surface staining on ice with Pacific Blue or eFluor450-anti-B220 (RA3-6B2), anti-CD11b (MI-70), anti-CD11c (N418), and anti-F4-80 (BM8) (Caltag); Pacific Orange-anti-CD8α (5H10) (Caltag); FITC-anti-CD27 (LG.7F9); APC-AlexaFluor 750 or APCeFluor780-anti-CD4 (RM4-5); PE-Cy7-anti-CD3ε (145-2C11), PE-anti-CD122 (5H4), and AlexaFluor 700-anti-CD44 (IM7) antibodies. For intracellular cytokine experiments, spleen and lymph node cells from challenged animals or *in vitro* stimulated cultures containing PMA(50 ng/ml), ionomycin (200 ng/ml), and brefeldin A (10 μg/ml, Sigma) underwent the tetramer enrichment and anti-CCR7 staining mentioned above in 10 μg/ml brefeldin A-containing buffer (Sigma) to prevent cytokine secretion. The enriched cells were surface stained with combinations of antibodies listed above then treated with BD Cytofix/Cytoperm, and then stained with PE-Cy7-anti-IFN-γ (XMG1.2) or PE-anti-IL-17A (TC11-18H10) (BD Pharmingen). In some experiments, the enriched cells were surface stained, then treated with eBioscience Foxp3 Fixation/Permeabilization Concentrate and Diluent, and stained with PE-anti-T-bet (eBio 4B10) or PE-anti-RORγt (AFKJS-9), or with BD Cytofix/Cytoperm and stained with PE-anti-Bcl-2 (3F11) (BD Pharmingen). In cases where BrdU labeling was performed, the enriched cells were surface stained and incorporated BrdU was detected with the BrdU Flow kit (BD Pharmingen) according to the manufacturer's specifications (BD Pharmingen). In all cases, the cells were then analyzed on an LSR II flow cytometer (Becton Dickinson). Data were analyzed with FlowJo software (TreeStar).

Memory cell transfer

Spleen and lymph nodes were collected from B6 mice infected at least 20 days earlier with LM-2W1S. For $CD27^-$ transfers, samples were depleted of $CD27^+$ cells (95–97% purity) using biotin-anti-CD27, anti-biotin beads (Miltenyi), and LD columns (Miltenyi). For $CD27^+$ transfers, samples were enriched for $CD4^+$ memory cells by adding 0.1 μg/ml biotin-anti-CD45RB to the biotin-labeled antibody cocktail provided in the Miltenyi CD4 Isolation kit and removing the biotin-labeled cells on an LS column. The remaining cells were stained with fluorochrome-labeled anti-CD44 and anti-CD27 prior to sorting $CD44^+$ $CD27^+$ events using a Becton Dickinson FACSAria. The purified cells were injected intravenously into B6.PL-$Thy1^a$ recipients. One or 14 d later, spleen and lymph node cells from the recipients were harvested, stained for 2W1S:I-A^b–SA-APC tetramer and Percp-Cy5.5-anti-CCR7 (4B12) for 1 h at 25°C, then with PE-anti-CD90.2 (53-2.1) and anti-PE magnetic beads. Bead bound cells were then stained with the non-T lineage-specific; anti-CD8α; anti-CD4; anti-CD27; and anti-CD44 antibodies listed above and the cells were then analyzed on an LSR II flow cytometer (Becton Dickinson). Data were analyzed with FlowJo software (TreeStar).

Statistical analysis

Differences between data sets were analyzed by paired or unpaired two-tailed Student's *t*-test. In Figure 3 a two-way ANOVA with a Bonferroni post-test was used to determine significance.

Acknowledgments

We thank S. Jameson, H. Chu and J. Taylor (University of Minnesota) for reviewing the manuscript, J. Walter, J. McLachlan and A. Schmidt for technical assistance, and P. Champoux and N. Shah for FACS sorting. Supported by grants from the US National Institutes of Health (AI39614, AI66016, and AI27998 to M. K. J.; T32-AI07313 to A. J. P., and T32-CA9138 to M. P.).

References

1. Jenkins MK, et al. In vivo activation of antigen-specific CD4 T cells. Annu Rev Immunol. 2001; 19:23–45. [PubMed: 11244029]
2. Ahmed R, Gray D. Immunological memory and protective immunity: understanding their relation. Science. 1996; 272:54–60. [PubMed: 8600537]
3. Sallusto F, Lenig D, Forster R, Lipp M, Lanzavecchia A. Two subsets of memory T lymphocytes with distinct homing potentials and effector functions. Nature. 1999; 401:708–712. [PubMed: 10537110]
4. Masopust D, Vezys V, Marzo AL, Lefrancois L. Preferential localization of effector memory cells in nonlymphoid tissue. Science. 2001; 291:2413–2417. [PubMed: 11264538]
5. Reinhardt RL, Khoruts A, Merica R, Zell T, Jenkins MK. Visualizing the generation of memory CD4 T cells in the whole body. Nature. 2001; 410:101–105. [PubMed: 11242050]
6. Seder RA, Ahmed R. Similarities and differences in $CD4^+$ and $CD8^+$ effector and memory T cell generation. Nat Immunol. 2003; 4:835–842. [PubMed: 12942084]
7. Zhou L, Chong MM, Littman DR. Plasticity of $CD4^+$ T cell lineage differentiation. Immunity. 2009; 30:646–655. [PubMed: 19464987]
8. Reiner SL, Locksley RM. The regulation of immunity to Leishmania Major. Annu Rev Immunol. 1995; 13:151–177. [PubMed: 7612219]

9. Swain SL, Hu H, Huston G. Class II-independent generation of CD4 memory T cells from effectors. Science. 1999; 286:1381–1383. [PubMed: 10558997]
10. Lohning M, et al. Long-lived virus-reactive memory T cells generated from purified cytokine-secreting T helper type 1 and type 2 effectors. J Exp Med. 2008; 205:53–61. [PubMed: 18195073]
11. Li J, Huston G, Swain SL. IL-7 promotes the transition of CD4 effectors to persistent memory cells. J Exp Med. 2003; 198:1807–1815. [PubMed: 14676295]
12. Hataye J, Moon JJ, Khoruts A, Reilly C, Jenkins MK. Naive and memory $CD4^+$ T cell survival controlled by clonal abundance. Science. 2006; 312:114–116. [PubMed: 16513943]
13. Marzo AL, et al. Initial T cell frequency dictates memory $CD8^+$ T cell lineage commitment. Nat Immunol. 2005; 6:793–799. [PubMed: 16025119]
14. Badovinac VP, Haring JS, Harty JT. Initial T cell receptor transgenic cell precursor frequency dictates critical aspects of the $CD8^+$ T cell response to infection. Immunity. 2007; 26:827–841. [PubMed: 17555991]
15. Rees W, et al. An inverse relationship between T cell receptor affinity and antigen dose during $CD4^+$ T cell responses in vivo and in vitro. Proc Natl Acad Sci USA. 1999; 96:9781–9786. [PubMed: 10449771]
16. Moon JJ, et al. Naive $CD4^+$ T cell frequency varies for different epitopes and predicts repertoire diversity and response magnitude. Immunity. 2007; 27:203–213. [PubMed: 17707129]
17. Ertelt JM, et al. Selective priming and expansion of antigen-specific $Foxp3^-$ $CD4^+$ T cells during *Listeria monocytogenes* infection. J Immunol. 2009; 182:3032–3038. [PubMed: 19234199]
18. Muller WJ, et al. Recombinant *Listeria monocytogenes* expressing an immunodominant peptide fails to protect after intravaginal challenge with herpes simplex virus-2. Arch Virol. 2008; 153:1165–1169. [PubMed: 18443737]
19. Portnoy DA, Auerbuch V, Glomski IJ. The cell biology of *Listeria monocytogenes* infection: the intersection of bacterial pathogenesis and cell-mediated immunity. J Cell Biol. 2002; 158:409–414. [PubMed: 12163465]
20. Moon JJ, et al. Tracking epitope-specific T cells. Nat Protoc. 2009; 4:565–581. [PubMed: 19373228]
21. Kaech SM, Hemby S, Kersh E, Ahmed R. Molecular and functional profiling of memory CD8 T cell differentiation. Cell. 2002; 111:837–851. [PubMed: 12526810]
22. Khoruts A, Mondino A, Pape KA, Reiner SL, Jenkins MK. A natural immunological adjuvant enhances T cell clonal expansion through a CD28-dependent, interleukin (IL)-2-independent mechanism. J Exp Med. 1998; 187:225–236. [PubMed: 9432980]
23. Pape KA, Merica R, Mondino A, Khoruts A, Jenkins MK. Direct evidence that functionally impaired $CD4^+$ T cells persist in vivo following induction of peripheral tolerance. J Immunol. 1998; 160:4719–4729. [PubMed: 9590217]
24. Szabo SJ, et al. A novel transcription factor, T-bet, directs Th1 lineage commitment. Cell. 2000; 100:655–669. [PubMed: 10761931]
25. Ivanov II, et al. The orphan nuclear receptor RORγt directs the differentiation program of proinflammatory $IL\text{-}17^+$ T helper cells. Cell. 2006; 126:1121–1133. [PubMed: 16990136]
26. Woolard MD, Hensley LL, Kawula TH, Frelinger JA. Respiratory Francisella tularensis live vaccine strain infection induces Th17 cells and prostaglandin E_2, which inhibits generation of gamma interferon-positive T cells. Infect Immun. 2008; 76:2651–2659. [PubMed: 18391003]
27. Zhang Z, Clarke TB, Weiser JN. Cellular effectors mediating Th17-dependent clearance of pneumococcal colonization in mice. J Clin Invest. 2009; 119:1899–1909. [PubMed: 19509469]
28. Park HS, et al. Primary induction of CD4 T cell responses in nasal associated lymphoid tissue during group A streptococcal infection. Eur J Immunol. 2004; 34:2843–2853. [PubMed: 15368301]
29. Hikono H, et al. Activation phenotype, rather than central- or effector-memory phenotype, predicts the recall efficacy of memory $CD8^+$ T cells. J Exp Med. 2007; 204:1625–1636. [PubMed: 17606632]
30. Snyder CM, et al. Memory inflation during chronic viral infection is maintained by continuous production of short-lived, functional T cells. Immunity. 2008; 29:650–659. [PubMed: 18957267]

31. Hendriks J, et al. CD27 is required for generation and long-term maintenance of T cell immunity. Nat Immunol. 2000; 1:433–440. [PubMed: 11062504]
32. Hendriks J, Xiao Y, Borst J. CD27 promotes survival of activated T cells and complements CD28 in generation and establishment of the effector T cell pool. J Exp Med. 2003; 198:1369–1380. [PubMed: 14581610]
33. Dolfi DV, et al. Late signals from CD27 prevent Fas-dependent apoptosis of primary $CD8^+$ T cells. J Immunol. 2008; 180:2912–2921. [PubMed: 18292513]
34. Rubinstein MP, et al. Converting IL-15 to a superagonist by binding to soluble IL-15Rα. Proc Natl Acad Sci USA. 2006; 103:9166–9171. [PubMed: 16757567]
35. Tokoyoda K, et al. Professional memory $CD4^+$ T lymphocytes preferentially reside and rest in the bone marrow. Immunity. 2009; 30:721–730. [PubMed: 19427242]
36. Weaver CT, Harrington LE, Mangan PR, Gavrieli M, Murphy KM. Th17: an effector CD4 T cell lineage with regulatory T cell ties. Immunity. 2006; 24:677–688. [PubMed: 16782025]
37. Korn T, Bettelli E, Oukka M, Kuchroo VK. IL-17 and Th17 Cells. Annu Rev Immunol. 2009; 27:485–517. [PubMed: 19132915]
38. Sato A, et al. $CD11b^+$ Peyer's patch dendritic cells secrete IL-6 and induce IgA secretion from naive B cells. J Immunol. 2003; 171:3684–3690. [PubMed: 14500666]
39. Kelsall B. Recent progress in understanding the phenotype and function of intestinal dendritic cells and macrophages. Mucosal Immunol. 2008; 1:460–469. [PubMed: 19079213]
40. Reis e Sousa C, et al. In vivo microbial stimulation induces rapid CD40 ligand-independent production of interleukin 12 by dendritic cells and their redistribution to T cell areas. J Exp Med. 1997; 186:1819–1829. [PubMed: 9382881]
41. Hsieh CS, Heimberger AB, Gold JS, O'Garra A. Development of T_H1 $CD4^+$ T cells through IL-12 produced by *Listeria*-induced macrophages. Science. 1992; 260:547–549. [PubMed: 8097338]
42. Homann D, Teyton L, Oldstone MB. Differential regulation of antiviral T-cell immunity results in stable $CD8^+$ but declining $CD4^+$ T-cell memory. Nat Med. 2001; 7:913–919. [PubMed: 11479623]
43. Monack DM, Mueller A, Falkow S. Persistent bacterial infections: the interface of the pathogen and the host immune system. Nat Rev Microbiol. 2004; 2:747–765. [PubMed: 15372085]
44. Surh CD, Sprent J. Homeostasis of naive and memory T cells. Immunity. 2008; 29:848–862. [PubMed: 19100699]
45. Allam A, et al. The $CD8^+$ memory T-cell state of readiness is actively maintained and reversible. Blood. 2009; 114:2121–2130. [PubMed: 19617575]
46. Kraus ZJ, Haring JS, Bishop GA. TNF receptor-associated factor 5 is required for optimal T cell expansion and survival in response to infection. J Immunol. 2008; 181:7800–7809. [PubMed: 19017969]
47. Intlekofer AM, et al. Effector and memory $CD8^+$ T cell fate coupled by T-bet and eomesodermin. Nat Immunol. 2005; 6:1236–1244. [PubMed: 16273099]
48. Joshi NS, et al. Inflammation directs memory precursor and short-lived effector $CD8^+$ T cell fates via the graded expression of T-bet transcription factor. Immunity. 2007; 27:281–295. [PubMed: 17723218]
49. Soares H, et al. A subset of dendritic cells induces $CD4^+$ T cells to produce IFN-γ by an IL-12-independent but CD70-dependent mechanism in vivo. J Exp Med. 2007; 204:1095–1106. [PubMed: 17438065]
50. Keller AM, Schildknecht A, Xiao Y, van den Broek M, Borst J. Expression of costimulatory ligand CD70 on steady-state dendritic cells breaks $CD8^+$ T cell tolerance and permits effective immunity. Immunity. 2008; 29:934–946. [PubMed: 19062317]
51. van Oosterwijk MF, et al. CD27-CD70 interactions sensitise naive $CD4^+$ T cells for IL-12-induced T_h1 cell development. Int Immunol. 2007; 19:713–718. [PubMed: 17548342]
52. Yang XO, et al. T helper 17 lineage differentiation is programmed by orphan nuclear receptors RORα and RORγ. Immunity. 2008; 28:29–39. [PubMed: 18164222]
53. Ribot JC, et al. CD27 is a thymic determinant of the balance between interferon-γ- and interleukin 17-producing γδ T cell subsets. Nat Immunol. 2009; 10:427–436. [PubMed: 19270712]

54. Lu YJ, et al. Interleukin-17A mediates acquired immunity to pneumococcal colonization. PLoS Pathog. 2008; 4:e1000159. [PubMed: 18802458]

55. Yamanaka N, Hotomi M, Billal DS. Clinical bacteriology and immunology in acute otitis media in children. J Infect Chemother. 2008; 14:180–187. [PubMed: 18574652]

56. Stoklasek TA, Schluns KS, Lefrancois L. Combined IL-15/IL-15Ralpha immunotherapy maximizes IL-15 activity in vivo. J Immunol. 2006; 177:6072–6080. [PubMed: 17056533]

57. Boggs DR. The total marrow mass of the mouse: a simplified method of measurement. Am J Hematol. 1984; 16:277–286. [PubMed: 6711557]

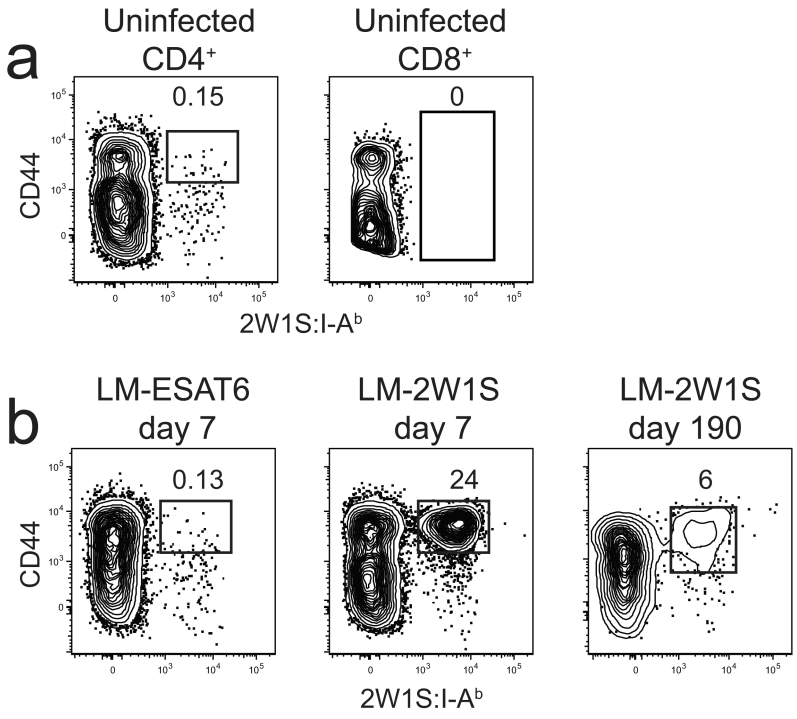

Figure 1.

Infection with LM-2W1S induces the clonal expansion of 2W1S:I-A^b-specific memory cells. $CD4^+$ or $CD8^+$ T cells were identified in enriched fractions by flow cytometry from $CD11c^-$ $CD11b^-$ $F4/80^-$ $B220^-$ $CD3^+$ gated events. (**a**) $CD4^+$ T cells (left) or $CD8^+$ T cells (right) from an uninfected B6 mouse with gates on $CD44^{high}$ 2W1S:I-A^{b+} (left) or all 2W1S:I-A^{b+} cells (right). (**b**) $CD4^+$ T cells in enriched samples from a B6 mouse 7 days after intravenous infection with LM-ESAT6 (left) or 7 (middle) or 190 (right) days after intravenous LM-2W1S infection. The percentages of cells in the indicated gates are shown. The plots are representative of greater than twenty (**a**) or 2-5 independent experiments (**b**).

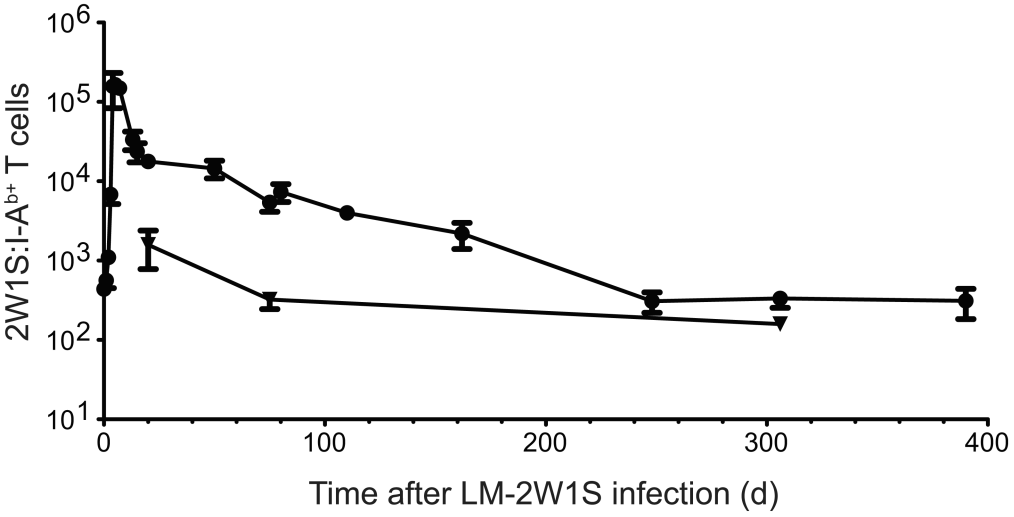

Figure 2.

2W1S:I-A^b-specific CD4$^+$ memory T cells decay after infection with LM-2W1S. Mean number of CD4$^+$ 2W1S:I-A^{b+} T cells ± SD ($n \geq 3$ for each data point) in the spleen and lymph nodes (circles) or bone marrow (triangles) after intravenous infection with LM-2W1S. A non-linear regression fit of the spleen and lymph node data yielded a $T_{1/2}$ of 43 days ($R^2 = 0.94$, 95% confidence interval of 30 – 73 days) for points between days 20 and 248.

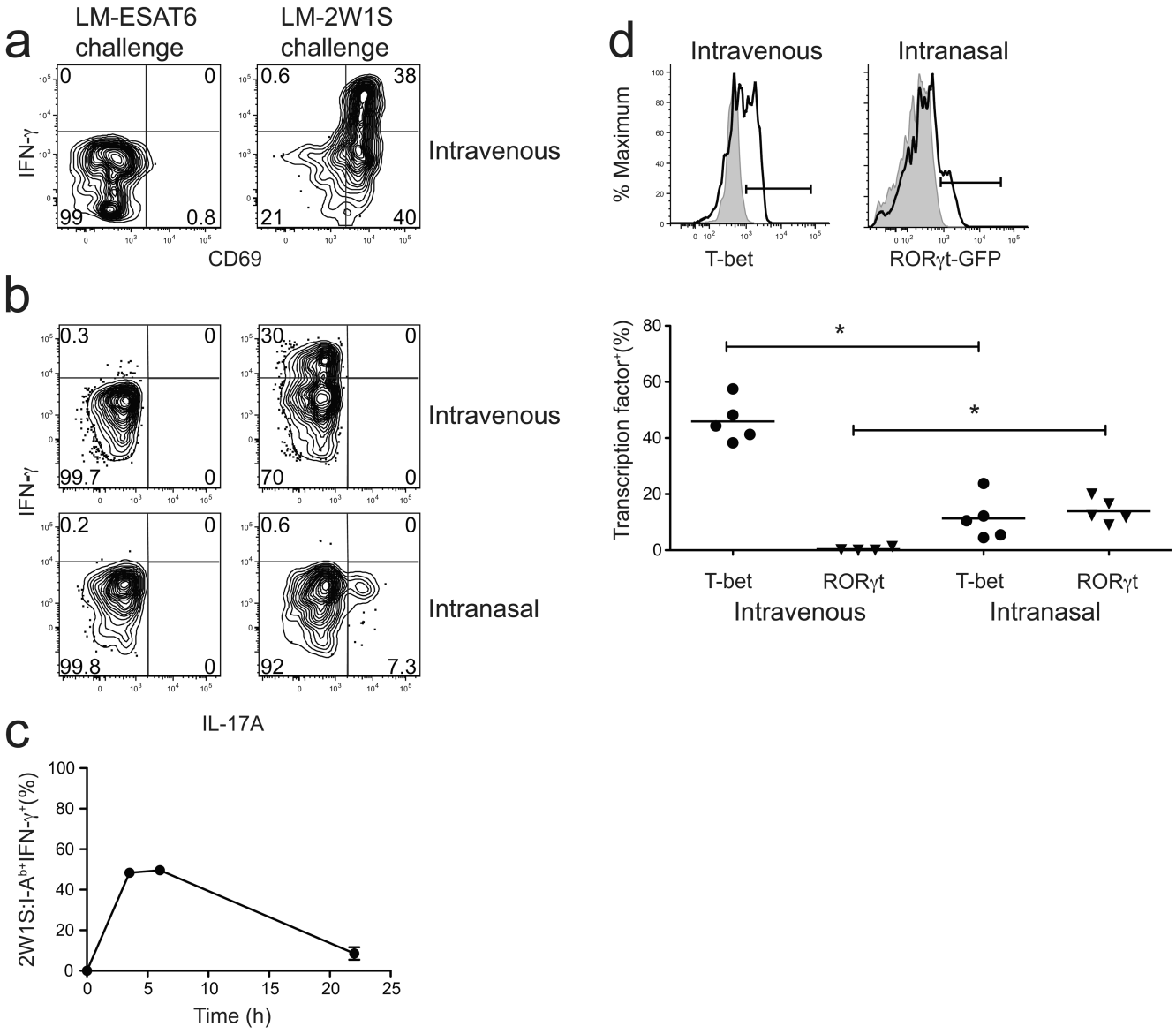

Figure 3.

Lymphokine production by 2W1S:I-A^b-specific $CD4^+$ memory T cells. CD69 expression (**a**), IFN-γ (**a,b**), and IL-17A production (**b**) by 2W1S:I-A^b-specific memory T cells, 2 h after challenge with LM-ESAT6 (left) or LM-2W1S (right). 2W1S:I-A^b-specific memory T cells were induced by intravenous (**a,b**) or intranasal (**b**) infection. (**c**) Percent of 2W1S:I-A^b-specific IFN-γ^+ $CD4^+$ memory T cells after stimulation with PMA and ionomycin in the presence of brefeldin A for 3.5 h, 6 h, or 22 h. (**d**, top) T-bet expression (left) in 2W1S:I-A^b-specific memory T cells (black line) induced by intravenous infection compared to $CD44^+$ $CD4^+$ T-bet deficient cells (gray histogram). eGFP expression in *Rorc*$(\gamma t)^{+/GFP}$ mice after intranasal infection (right) in 2W1S:I-A^b-specific memory T cells (black line) compared to wild-type 2W1S:I-A^b-specific memory T cells (gray histogram) after intranasal infection. (**d**, bottom) Scatter plot showing the percentage of T-bet^+ or RORγt^+ 2W1S:I-A^b-specific memory T cells in individual mice based on the gates in (**d**, top) (asterisk, $P < .01$ for T-bet

samples, $P < 0.05$ for RORγt samples). Plots are representative of three (**a**), six (**b**), two (**c**) or four independent experiments examining T-bet and RORγt expression by intracellular staining and one with *Rorc*(*γt*)$^{+/GFP}$ mice (**d**).

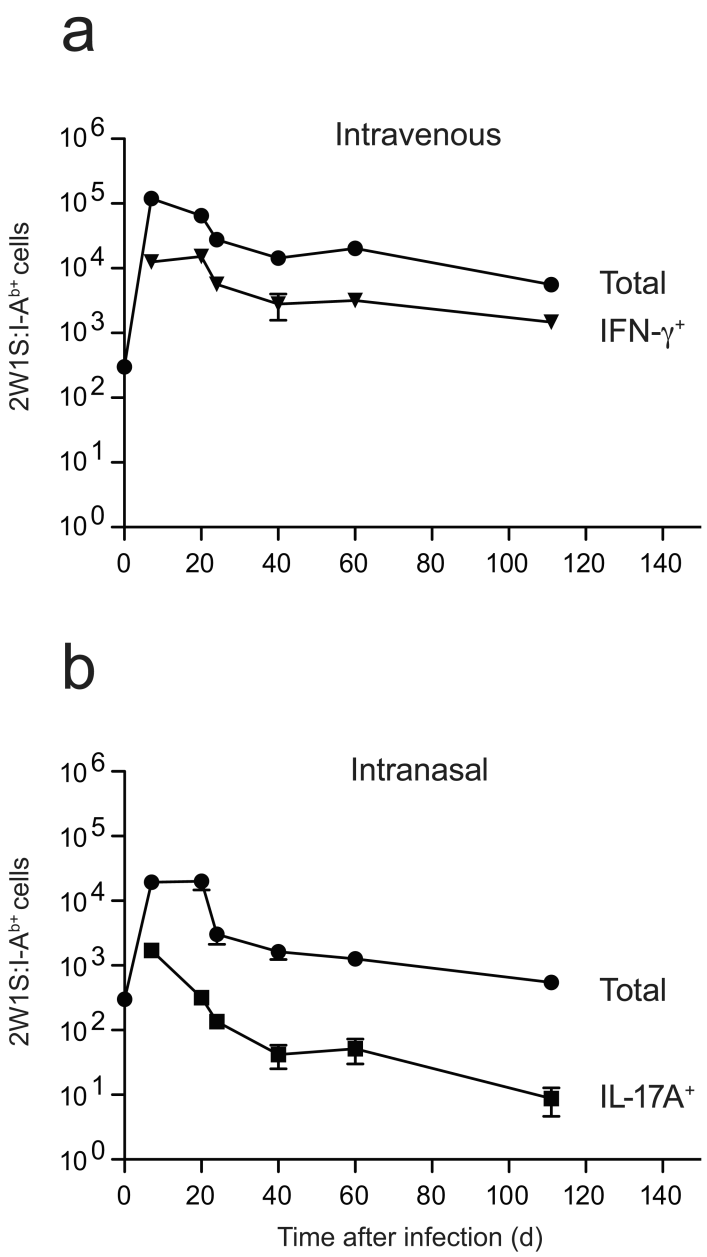

Figure 4.

Survival of IFN-γ and IL-17A-producing 2W1S:I-A^b-specific $CD4^+$ memory T cells. Mean number (± SD, n = 3–5 at each time point) of total 2W1S:I-A^b-specific $CD4^+$ T cells (circles) induced by intravenous (**a**) or intranasal (**b**) infection and 2W1S:I-A^b-specific $CD4^+$ T cells that made IFN-γ but not IL-17A (**a**, triangles) or IL-17A but not IFN-γ (**b**, squares) after challenge with LM-2W1S.

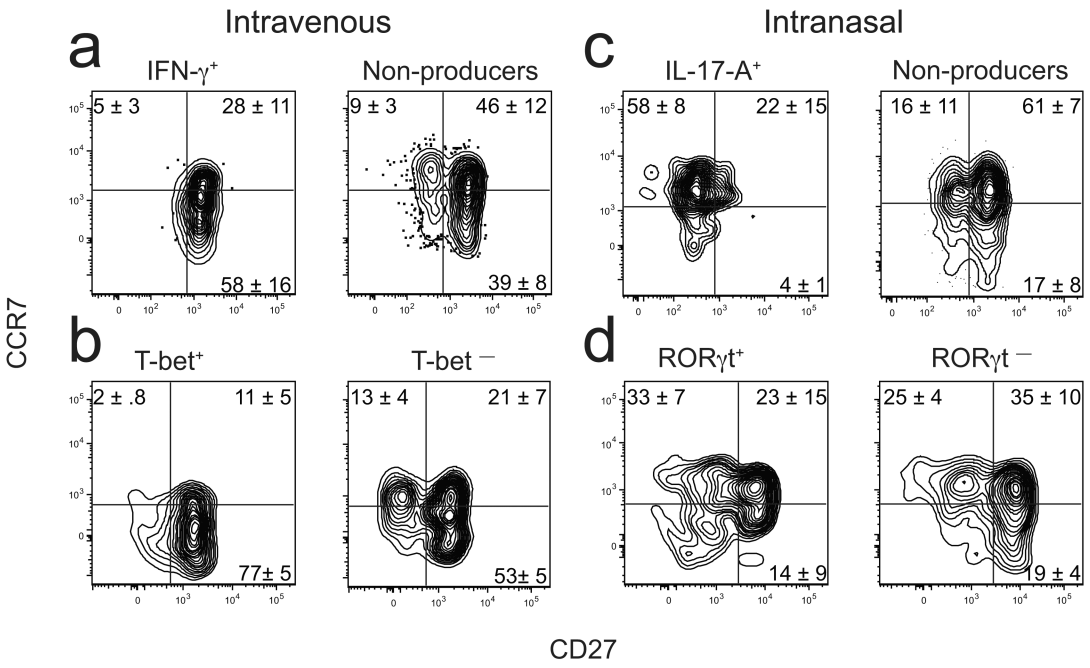

Figure 5.

Surface phenotype of 2W1S:I-A^{b}-specific T cells. Representative plot of CCR7 and CD27 expression on 2W1S:I-A^{b}-specific T cells in mice at least 20 days after intravenous (**a,b**) or intranasal (**c,d**) infection.The quadrant lines were based on 2WIS:I-A^{b-} CD44^{low} naive cells in each sample. This population was uniformly CCR7^{high} and contained CD27^{low} and CD27^{high} subsets. The horizontal line was set at the lowest level of CCR7 on the entire population and the vertical line at the midpoint between the CD27^{low} and CD27^{high} subsets. (**a**) Cells that produced IFN-γ but not IL-17A (left) or neither (right) after challenge with LM-2W1S. (**b**) T-bet^{+} (left) or T-bet $^{-}$ (right) antigen-experienced cells without challenge (**c**) Cells that produced IL-17A but not IFN-γ (left) or neither (right) after challenge with LM-2W1S. (**d**) RORγt^{+} (left) or RORγt $^{-}$ (right) antigen-experienced cells without challenge. The values on the plots represent the mean percentage of cells (± SD, $n \geq 4$) in the indicated quadrants. Data are representative of seven (**a**), four (**b**), six (**c**), or two independent experiments (**d**).

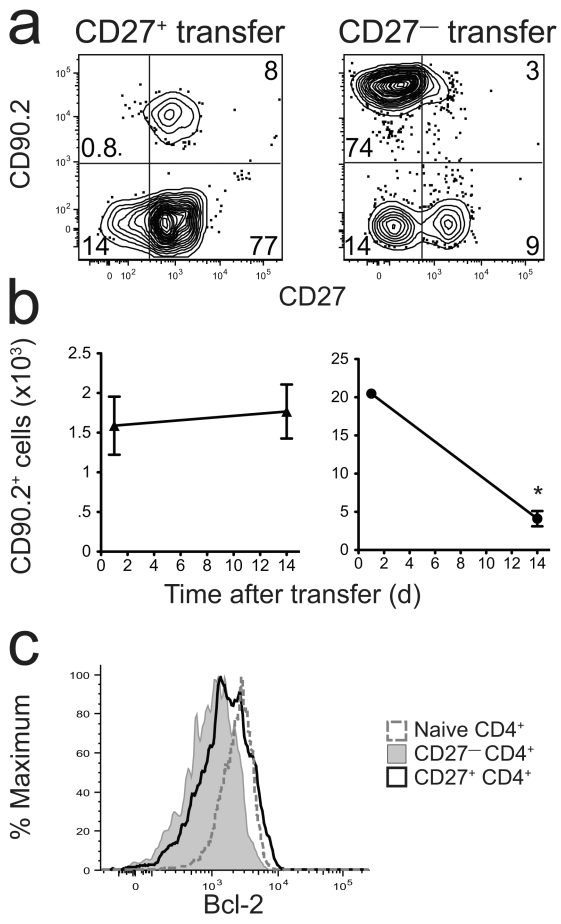

Figure 6.

CD27^{-} CD4^{+} memory T cells are short-lived. (**a**) Representative contour plots of CD90.2-enriched fractions of spleen and lymph node cells from mice that received purified CD90.2^{+} CD27^{+} (left) or CD27^{-} (right) total CD4^{+} memory T cells one day earlier. (**b**) Mean number (± SD, *n* = 3-4) of CD90.2^{+} CD27^{+} (left) or CD27^{-} (right) cells recovered 1 or 14 days after transfer into B6.PL-Thy1^{a} recipients. The number of CD27^{-} cells recovered on day 14 was significantly lower than the number recovered on day 1, *P* = 0.0005 (asterisk). (**c**) Bcl-2 expression by total naïve CD4^{+} T cells (dashed line), or CD27^{-} (gray histogram) or CD27^{+} (black line) 2W1S:I-A^{b+} memory T cells. Data are representative of three (**a,b**) or two independent experiments (**c**).

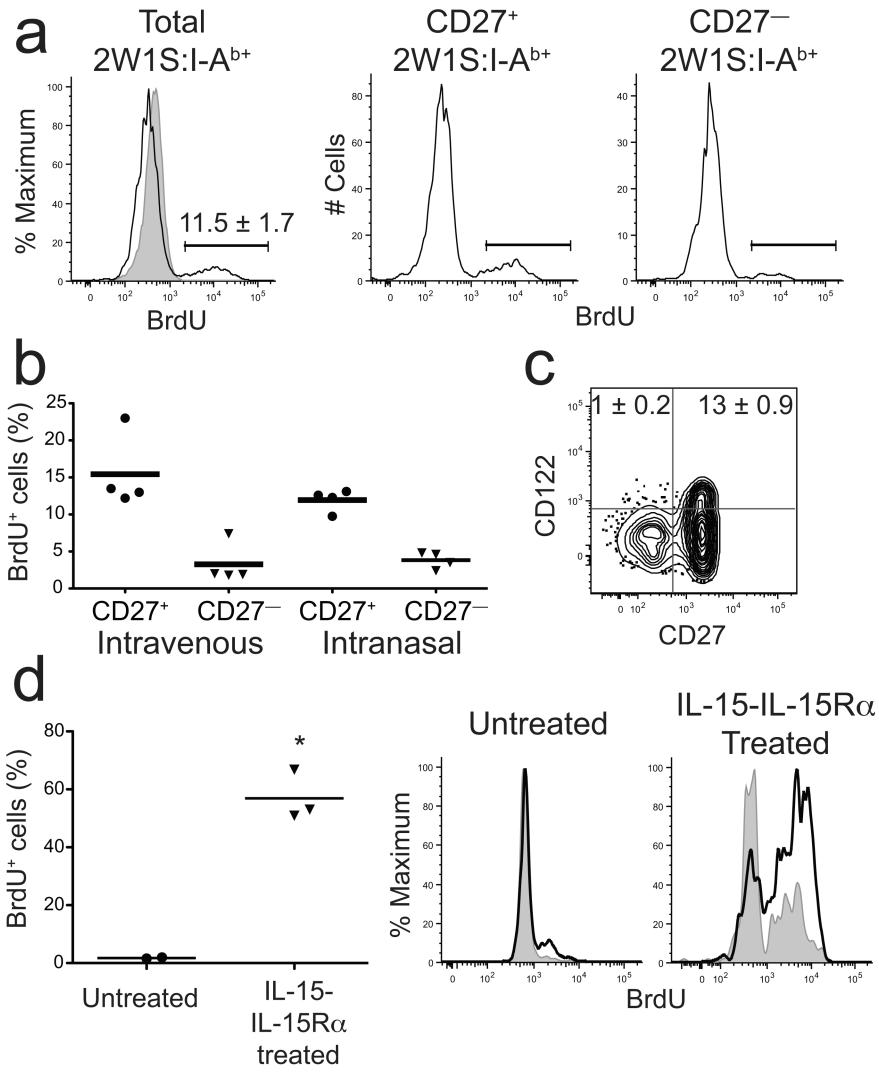

Figure 7.

CD4$^+$ memory T cells undergo limited homeostatic proliferation. (**a**) Representative BrdU histograms for total (left), CD27$^+$ (middle), or CD27$^-$ (right) 2W1S:I-A^{b+} CD4$^+$ memory cells in mice fed BrdU for 14 days beginning 40 days after intravenous LM-2W1S infection, along with a histogram of total CD4$^+$ T cells (gray) from a mouse that did not receive BrdU (left). Gates used to identify BrdU$^+$ cells are shown. (**b**) Scatterplot of the percentage of BrdU$^+$ 2W1S:I-A^{b+} CD4$^+$ memory T cells that were CD27$^+$ or CD27$^-$ in individual mice, based on the gates shown in (**a**). (**c**) Representative contour plot of CD122 and CD27 on 2W1S:I-A^{b+} CD4$^+$ memory T cells induced by intravenous infection. Mean percentages (± SD, n = 5) of CD122$^+$ cells are shown in the relevant quadrants. (**d**) Scatterplot of the percent BrdU$^+$ 2W1S:I-A^{b+} CD4$^+$ memory cells in individual mice that were not injected (circles) or injected with IL-15–IL-15Rα complexes (triangles) and given BrdU for 5 days beginning 20 days after intravenous LM-2W1S infection. BrdU$^+$ cells were identified as shown in (**a**). Representative histograms of BrdU incorporation by CD27$^+$ (solid line) or CD27$^-$ (gray) 2W1S:I-A^{b+} CD4$^+$ memory T cells in mice that were not injected (left) or

injected with IL-15–IL-15Rα complexes (right) and given BrdU for 5 days beginning 20 d after intravenous LM-2W1S infection. Horizontal bars on each scatter plot indicate the means for each population. The number of $BrdU^+$ cells in the IL-15–IL-15Rα complex-treated group was significantly greater than in the untreated group (asterisk, $P = 0.003$). Data are representative of three (**a,b**), two (**c**), one experiment (**d**).